Applied Catalysis B: Environmental 91 (2009) 262–268

Contents lists available at ScienceDirect

Applied Catalysis B: Environmental

journal homepage: www.elsevier.com/locate/apcatb

A comprehensive investigation of influences of NO and O_2 on N_2O-SCR by CH_4 over Fe-USY zeolite

Qun Shen [a], Landong Li [a], Chi He [a], Hua Tian [a], Zhengping Hao [a,*], Zhi Ping Xu [b,**]

[a] Department of Environmental Nano-materials, Research Center for Eco-Environmental Sciences, Chinese Academy of Sciences, Beijing 100085, PR China
[b] Australian Research Council (ARC) Centre of Excellence for Functional Nanomaterials, Australian Institute for Bioengineering and Nanotechnology and School of Engineering, The University of Queensland, Brisbane, QLD 4072, Australia

ARTICLE INFO

Article history:
Received 12 March 2009
Received in revised form 25 May 2009
Accepted 26 May 2009
Available online 6 June 2009

Keywords:
Fe-USY zeolite
N_2O–CH_4 SCR
NO inhibition
NO-assisted N_2O decomposition
N_2O–CO SCR

ABSTRACT

The catalytic reduction behaviors of N_2O by CH_4 have been investigated over Fe-USY catalyst by examining the influences of CH_4, NO, O_2, or their mixtures in detail. The observations show that NO and O_2, which inevitably exist in the gases emitted from industrial sources, such as the nitric acid plant, inhibit the selective catalytic reduction of N_2O by CH_4 (N_2O–CH_4 SCR) to some degree, shifting the temperature for >90% N_2O conversion to over 450 °C. The prohibition of O_2 can be ascribed to its occupying active sites and oxidizing CH_4-derived intermediates. The negative effect of NO is very prominent, inhibiting the N_2O conversion by strongly occupying the active sites and gradually moving the reaction pathways from N_2O–CH_4 SCR to NO-assisted N_2O decomposition, where the former is more efficient than the latter for N_2O decomposition under the same operation conditions. In addition, the amount of reducing agent CH_4 has also influenced the N_2O conversion profile.

1. Introduction

It has been reported that the global warming potential (GWP) per molecular N_2O is about 300 times as high as that of carbon dioxide [1] and the N_2O atmospheric concentration continues to increase at a rate of 0.25% per year [2], thus the greenhouse effect of N_2O becomes more and more significant via absorbing infrared radiation in the atmosphere. More severely, N_2O can destruct the stratospheric zone layer, allowing more UV light to reach the earth surface and causing various human health diseases. Therefore, the abatement of nitrous oxide is of great urgency.

At current, catalytic decomposition of N_2O and selective catalytic reduction (SCR) of N_2O with reducing agents are two most-common choices. To this end, various kinds of catalysts, such as metal oxides [3–5], supported noble metals [6] and transition metal-exchanging zeolites (Co–zeolite, Fe–zeolite, etc.) [7–13], have been intensively investigated for N_2O direct decomposition. In particular, the addition of a reducing agent into the gas mixture can facilitate the removal of surface oxygen (i.e. the rate-limiting step in N_2O direct decomposition) and thus decrease the reaction operation temperature [14–20]. Therefore, SCR of N_2O with a reducing agent is recently considered as a promising technology to abate nitrous oxide in real conditions. Among various reductants (CO, H_2, NH_3, hydrocarbons, etc.), methane shows a high reducing capability [21,22], and enables SCR of N_2O to readily proceed at a lower temperature (<400 °C) over Fe-exchanged zeolite (BEA, MFI, etc.) even in the presence of excess O_2 [16,21,22]. Methane is the main component of natural gas and also present in some combustion exhaust. Compared with NH_3-SCR of N_2O, CH_4 SCR is more advantageous in transportation, storage, equipment corrosion, etc. Therefore, CH_4 SCR of N_2O is thought as a practical method to eliminate N_2O in terms of the efficiency and the cost.

The effect of CO and/or NO on N_2O direct decomposition over zeolite catalysts has been investigated in detail by Pérez-Ramírez et al. [23,24]. However, to our knowledge, recent studies about N_2O–CH_4 SCR are mostly focused on Fe-Beta and Fe-MFI catalysts to understand the CH_4 activation mechanism in N_2O-SCR [25–28], and there is no report about how SCR of N_2O by CH_4 is affected by the co-existence NO, O_2 and/or H_2O that are inevitably present in the N_2O emission site, such as the nitric acid and adipic acid factories. Although most zeolite catalysts suffer the activity loss during the operation under these practical conditions, we have luckily found that Fe-USY zeolite shows a high activity and a high hydrothermal stability for N_2O decomposition in our previous studies under the similar conditions [11,12]. Therefore, the objective of this paper was to examine the catalytic behaviors of N_2O–CH_4 SCR in the presence of NO and/or O_2 over the potential effective catalyst (Fe-USY) in order to understand the N_2O decomposition mechanism in different reaction environments.

* Corresponding author. Tel.: +86 10 62849194; fax: +86 10 62923564.
** Corresponding author. Tel.: +61 7 33463809; fax: +61 7 33463973.
E-mail addresses: zpinghao@rcees.ac.cn (Z. Hao), gordonxu@uq.edu.au (Z.P. Xu).

0926-3373/$ – see front matter © 2009 Elsevier B.V. All rights reserved.
doi:10.1016/j.apcatb.2009.05.034

2. Experimental

Commercial ultra-stable Y (H-USY, Si/Al = 11.6, surface area = 512.4 m^2/g) was provided by Sinopec Co. and directly used as the parent zeolite in this study. The parent zeolite (*ca.* 5 g) was added into 500 ml 0.05 M $FeCl_3$ aqueous solution, and the ion exchange was carried out under vigorous stirring for 48 h at room temperature. After ion exchange, the zeolite was filtered, thoroughly washed with deionized water, dried at 100 °C overnight and then calcined at 600 °C for 4 h in air.

Temperature-programmed desorption (TPD) experiments were conducted on a Micromeritics Chemisorb 2720 apparatus. Prior to the TPD run, Fe-USY catalyst (0.10 g) was first treated in the reactor at 300 °C for 1 h and then cooled to room temperature in a stream of He. For O_2 adsorption, O_2 diluted with He (1%) was fed into the catalyst bed at room temperature for 0.5 h. Then the gas stream was switched to the pure He at a flow rate of 50 ml min^{-1} for 1 h to remove the physically adsorbed O_2. Afterward the sample was heated at a heating rate of 10 °C min^{-1} to 800 °C to desorb O_2 in He, and the effluent gas composition was analyzed online by a TCD detector. In addition, temperature-programmed desorption of NO (TPD-NO) over the Fe-USY catalyst was conducted similarly to O_2-TPD, while the effluent gas composition was analyzed by a Chemiluminescence NO–NO_2–NO_x analyzer (Model EC 9841, Ecotech Corporation).

The activity evaluation experiments of N_2O–CH_4 SCR using Fe-USY as the catalyst were performed in a fixed-bed flow microreactor at the atmospheric pressure. In each test, 0.10 g catalyst (sieve fraction: 0.25–0.5 mm) was placed into a quartz reactor (4 mm i.d.) and pretreated in He at 600 °C for 1 h. After the reactor was cooled down to 200 °C, the reactant gas mixture (N_2O, CH_4 and other gases, He balance) was fed into the catalytic reactor with the total flow rate at 60 ml min^{-1}, i.e. GHSV = ~30,000 h^{-1}. The effluent gas composition was analyzed online using a gas chromatograph (Agilent 6820 series) equipped with a TCD detector and two serial columns (a Porapak Q column served for separation of CH_4, N_2O, and CO_2, and a Molecular Sieve 5A column for separation of N_2, O_2, and CO). The steady-state activity data were recorded every 25 °C with ascending the reaction temperature from 200 to 600 °C.

3. Results

3.1. Physical characterization of zeolite catalyst

The as-prepared Fe-USY catalyst contains 3.38 wt% Fe, with Fe/Al ratio of 0.42, far more than the loading in other zeolites as prepared in this lab. The Fe-USY catalyst has a surface area of 528 m^2/g, similar to that of parent zeolite H-USY. After loading of Fe species, the zeolite structure has been well preserved. The nature and distribution of Fe species in USY, as previously assessed by UV–vis spectra, are mainly isolated ferric ions and oligonuclear iron clusters, as well as bulk iron oxide aggregates on the channel wall and/or the surface of USY. More detailed information about the structure of Fe-USY can be referred to our previous work [11,12].

3.2. N_2O-SCR with reducing agents and O_2

Fig. 1 shows the effect of reducing agents on N_2O decomposition over Fe-USY catalyst. The conversion profiles indicate that these reducing gases undoubtedly facilitate N_2O decomposition. In particular, N_2O conversion in N_2O-SCR by CH_4 is much higher than N_2O-SCR by NH_3 or CO, with >90% N_2O conversion attained below 400 °C in N_2O-SCR by CH_4, even in 5% O_2 stream (Fig. 1B). This observation is similar to the report by Nobukawa et al. that the reaction rate of N_2O reduction with CH_4 is higher than that with H_2 or CO over Fe-MFI [16]. Therefore, CH_4 is a favorable reducing agent in N_2O catalytic decomposition, and thus we focused our investigation on N_2O-SCR by CH_4 in the following sections.

3.3. N_2O–CH_4 SCR at varied CH_4/N_2O ratios

Fig. 2 shows the dependence of N_2O conversion to N_2 on the CH_4 concentration (0–2500 ppm). In comparison with the conversion curve without CH_4 added (black square), the curve with CH_4/N_2O = 0.25 shifts to the low temperature side by 70–80 °C within the conversion range of 10–90%. As CH_4/N_2O increases to 0.50, the conversion curve is almost overlapping that at CH_4/N_2O = 0.25, indicating that increasing the ratio CH_4/N_2O over 0.25 no longer facilitates N_2O decomposition. However, when CH_4/N_2O is less than 0.25, the facilitation effect is varied. For example, at CH_4/

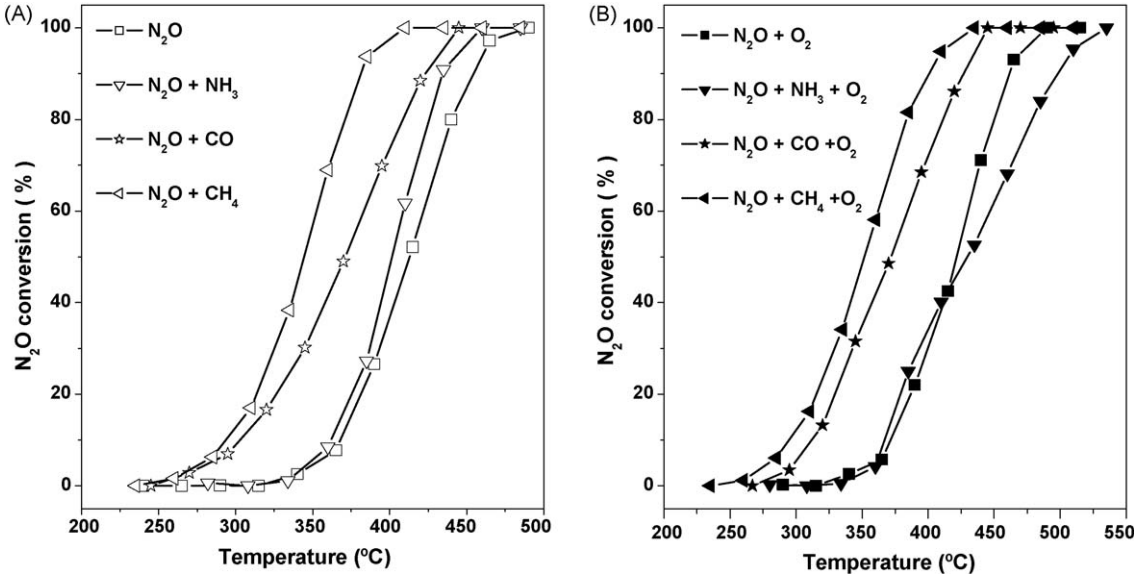

Fig. 1. Conversion profiles of N_2O-SCR by CH_4, CO, or NH_3 without O_2 (A) or with O_2 (B) over Fe-USY catalyst under reaction conditions: 0.10 g catalyst; 5000 ppm N_2O; 2000 ppm CH_4, 5000 ppm CO, or 4000 ppm NH_3; with or without 5% O_2, balance He; GHSV = 30,000 h^{-1}.

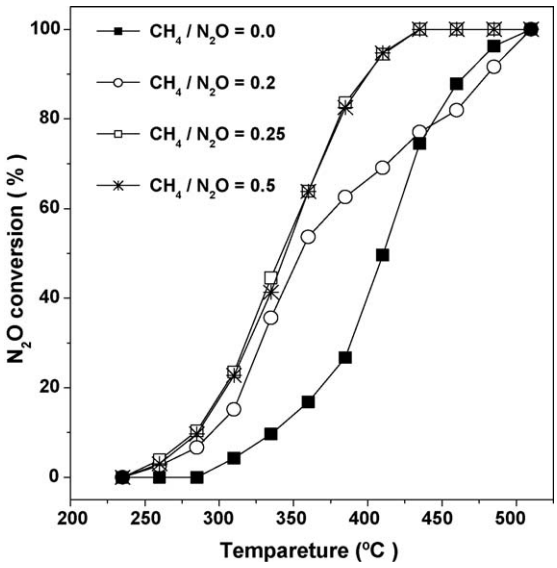

Fig. 2. N_2O conversion profiles over Fe-USY at different CH_4 concentrations under reaction conditions: 0.10 g catalyst; 5000 ppm N_2O; 0, 1000, 1250, or 2500 ppm CH_4, balance He; GSHV = 30,000 h^{-1}.

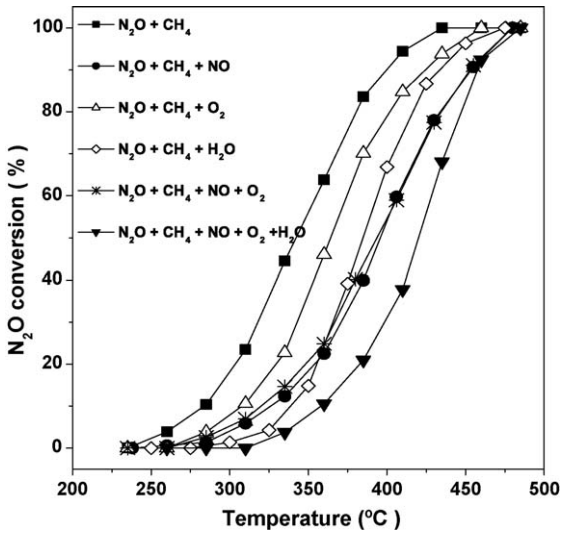

Fig. 4. N_2O conversion profiles over Fe-USY in different gas mixtures under reaction conditions: 0.10 g catalyst; 5000 ppm N_2O, 1750 ppm CH_4; and/or 700 ppm NO, and/or 5% O_2, and/or 2% H_2O, balance He; GSHV = 30,000 h^{-1}.

N_2O = 0.2, in the low temperature range, the N_2O conversion curve is only slight below that at CH_4/N_2O = 0.25. As the temperature increases to over 350 °C, the facilitation slows down, with the N_2O conversion being close to or even less than the conversion in N_2O direct decomposition (CH_4/N_2O = 0.0, Fig. 2), since there should be no CH_4 available when the conversion is more than 80%.

Our further investigation indicates that the generated CO and CO_2 amount is also dependent on the CH_4/N_2O ratio, as seen in Fig. 3. Given the reducibility of CH_4 is fully used to reduce N_2O, then one CH_4 will reduce four N_2O and produce one CO_2 (refer to (R4) in next section), and thus we can estimate the theoretical CO_2 amount from the conversion of N_2O, i.e. 1/4 of converted N_2O amount. As shown in Fig. 3A, when CH_4/N_2O is 0.20, CO_2 is first observed at 260 °C and its amount increases with the temperature until 435 °C, with the final concentration of *ca.* 1030 ppm, nearly equal to the CH_4 quantity (1000 ppm). On the other hand, CO is detected in a very small amount in 290–400 °C, with a maximum at 310–335 °C (Fig. 3D). When the ratio CH_4/N_2O = 0.25 and 0.50, as shown in Fig. 3B and C, the CO_2 concentration detected is lower than the theoretically calculated value by 300–400 (CH_4/N_2O = 0.25) or 500–700 ppm

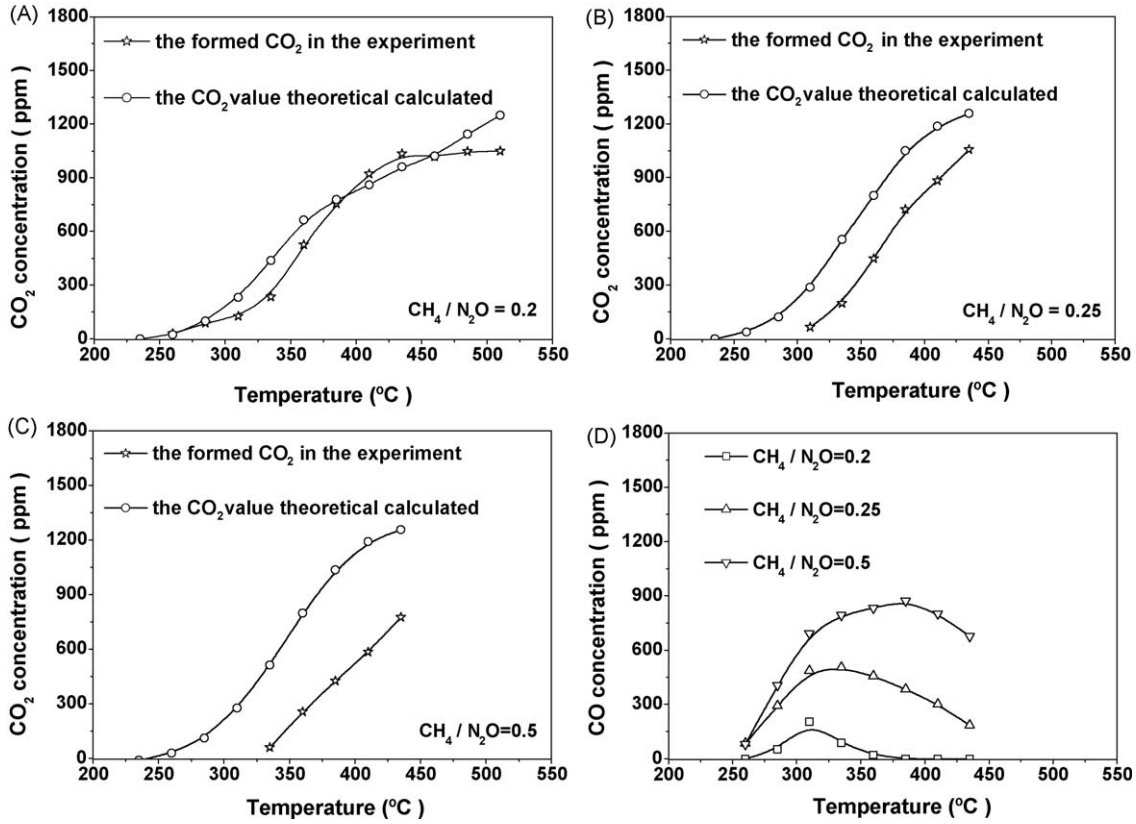

Fig. 3. CO and CO_2 profiles in N_2O-SCR by CH_4 under reaction conditions: 0.1 g catalyst; 5000 ppm N_2O; 0, 1000, 1250, or 2500 ppm CH_4; balance He; GHSV = 30,000 h^{-1}.

(CH_4/N_2O = 0.50) in 335–435 °C. However, the produced CO amount (Fig. 3D) is significantly increased at a larger CH_4/N_2O ratio, but similarly decreased at temperatures over 350–400 °C.

3.4. N_2O–CH_4 SCR in the co-existence of O_2, H_2O and/or NO

At the N_2O emission sites, other gases such as NO, O_2 and H_2O are inevitably present, and thus we need to understand their effects on the catalytic behaviors of N_2O-SCR by CH_4 over Fe-USY catalyst. As shown in Fig. 4, adding NO, O_2, H_2O or their mixtures to the $N_2O + CH_4$ stream all leads to a lower N_2O conversion at the same temperature. Individually, NO exhibits the strongest negative effect, followed by H_2O and then O_2. For example, the presence of 5% O_2 just shifts the conversion curve by ~25 °C to the high temperature side, indicating that N_2O–CH_4 SCR is slightly influenced by O_2, which is consistent with the report by Kameoka et al. [21]. The presence of 2% H_2O moves the conversion curve to the high temperature side by 40–50 °C, with its influence more severe in the low temperature range. As far as the NO influence is concerned, we can see that the curve moves to the higher temperature range by >50 °C in the presence of only 700 ppm NO.

Interestingly, the N_2O conversion in $N_2O + CH_4 + NO + O_2$ mixture system is almost identical to that in the $N_2O + CH_4 + NO$ mixture at the same temperature, probably due to masking of the negative effect of O_2 by NO. However, further adding H_2O to the $N_2O + CH_4 + NO + O_2$ reaction system leads to a further decrease of the N_2O conversion under the same conditions. As for the $N_2O + CH_4 + NO + O_2 + H_2O$ system, a simulated gas mixture emitted from the nitric acid plant, the N_2O conversion is about 20% less in 375–450 °C than that in the case without H_2O presence (Fig. 4). These observations may imply that the interference of O_2, NO and/or H_2O with N_2O–CH_4 SCR is different in terms of mechanism, which is probably revealed by the apparent activation energy shown in Fig. 5.

The apparent activation energies of N_2O decomposition in the presence of various gases have been estimated in the N_2O conversion range of 0–20% by assuming a plug-flow model and a first-order reaction, as shown in Fig. 5. Obviously, the apparent activation energy of N_2O–CH_4 SCR (88 kJ mol^{-1}) is much smaller than that of direct N_2O decomposition (139 kJ mol^{-1}) over Fe-USY. After adding NO and O_2, the apparent activation energy is increased by 15 and 8 kJ mol^{-1}, respectively. The apparent activation energy of $N_2O + CH_4 + NO$ and $N_2O + CH_4 + NO + O_2$ is almost the same, implying that the O_2 negative effect could be neglected in the NO co-presence and a similar reaction mechanism may proceed in both $N_2O + CH_4 + NO$ and $N_2O + CH_4 + NO + O_2$ reaction systems.

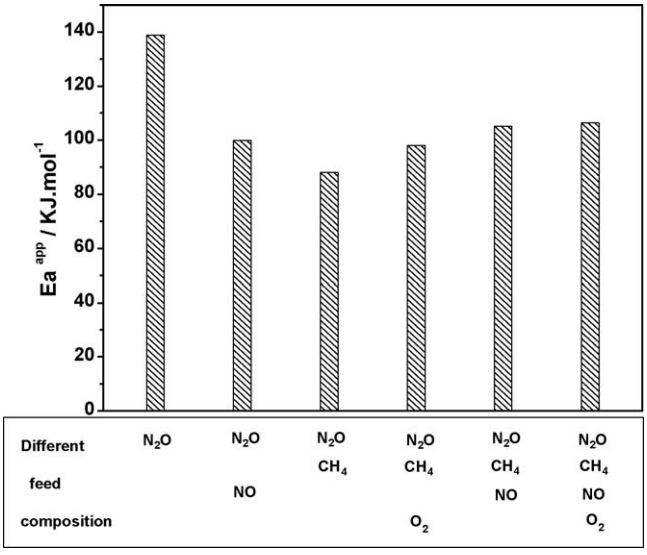

Fig. 5. Apparent activation energy (Ea^{app}) of N_2O decomposition over Fe-USY catalyst in various different gas compositions, with a standard deviation of 2 kJ mol^{-1}.

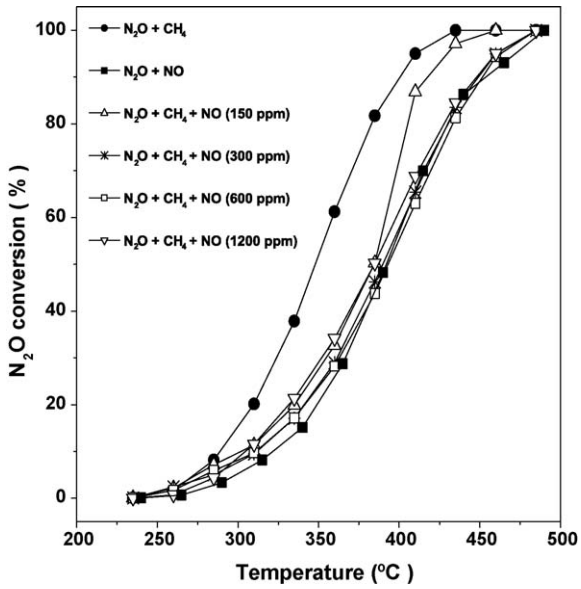

Fig. 6. The N_2O conversion profiles of N_2O-SCR by CH_4 under reaction conditions: 0.10 g catalyst; 5000 ppm N_2O; 1750 ppm CH_4; 150, 300, 600, or 1200 ppm NO, balance He; GHSV = 30,000 h^{-1}.

3.5. N_2O–CH_4 SCR in the presence of NO

Considering the severe negative effect of NO in N_2O-SCR by CH_4, we further examined N_2O–CH_4 SCR at different NO concentrations, as shown in Fig. 6. Very interestingly, the N_2O conversion is decreased to almost the same scale when NO concentration is varied in 300–1200 ppm, which is similar to the report by Boutarbouch et al. [23] that a small amount of NO is sufficient to severely inhibit reduction of N_2O with CO. Even at [NO] = 150 ppm, N_2O decomposition is similarly inhibited, and only at higher temperatures (400–450 °C) the inhibition gradually disappears, approaching to the profile of N_2O–CH_4 SCR. Note that at [NO] = 300–1200 ppm, the N_2O conversion profile nearly overlaps that of NO-assisted N_2O decomposition (black square in Fig. 6).

Further examinations reveal that the CH_4 consumption and the CO_2/CO formation are all affected by the NO partial pressure, as shown in Fig. 7. In general, the higher the NO partial pressure, the lower the CH_4 consumption. For example, at 440 °C, the CH_4 consumption is 70%, 68%, 45%, and 39% at [NO] = 0, 150, 600, and 1200 ppm, respectively. When there is no NO present, both CO_2 and CO are detected, where the CO_2 amount is increased with the increase of temperature while the CO amount reaches a maximum value at 300–350 °C and decreases with the increase of temperature afterwards. When NO is present, the generation of CO is severely prohibited and not detected at [NO] ≥600 ppm while the CO_2 formation is slightly less in the amount.

3.6. Catalyst stability

The durability test (Fig. 8) indicates that a slight catalytic activity loss is observed over 96 h at the selected temperatures, showing a relatively long stability. This observation indicates that the as-prepared Fe-USY shows promising as the effective catalyst for N_2O–CH_4 SCR by in the practical situation.

4. Discussion

4.1. The mechanism of N_2O-SCR by CH_4

In the $N_2O + CH_4 + NO + O_2$ reaction system, three oxidative gases can possibly react with CH_4. However, our experiments (Supplementary Figures S1 and S2) indicate that NO or O_2 can only react with CH_4 to produce a limited amount of CO_2 and CO in 250–500 °C over Fe-USY catalyst, different from that CH_4 can facilitate the SCR of NO over Co-ZSM-5 zeolite catalyst [9,29]. This suggests that CH_4 can only be activated by N_2O over Fe-USY catalyst in the $N_2O + CH_4 + NO + O_2$ reaction system. The facilitation of CH_4 to N_2O decomposition has been proposed by Nobukawa et al. via the following reactions based on their detail IR investigation [28]:

$$Fe{-}OH + CH_4 + N_2O \rightarrow Fe{-}OCH_3 + H_2O + N_2 \quad (R1)$$

$$Fe{-}OCH_3 + 2N_2O \rightarrow Fe{-}OOCH + H_2O + 2N_2 \quad (R2)$$

$$Fe{-}OOCH + N_2O \rightarrow Fe{-}OH + CO_2 + N_2 \quad (R3)$$

$$Sum: 4N_2O + CH_4 \rightarrow CO_2 + 4N_2 + 2H_2O \quad (R4)$$

Firstly, CH_4 is only activated by N_2O on the Fe–OH active sites, completely dependent on the simultaneous presence of N_2O and CH_4 (R1). Nobukawa et al. [25,26,28] found that the simultaneous presence of CH_4 and N_2O is essential for the high SCR activity. They proposed that some oxygen species dissociated from N_2O are highly reactive (nascent) but some non-reactive (thermally accommodated). The highly reactive (nascent) oxygen species can be formed only in the simultaneous presence of CH_4 and N_2O, which subsequently oxidizes CH_4 (R1) [25,26,28,30]. The intermediate Fe–OCH_3 species is then oxidized preferentially by N_2O to form Fe–OOCH (R2). Finally, the oxidation of Fe–OOCH by N_2O (R3) continues in a much easier way, producing CO_2 and regenerating the Fe–OH active sites [28].

In addition, Wood et al. [31] observed that during oxidation of CH_4 to CH_3OH over Fe/Al-FMI by N_2O, a minor amount of CO is detected. They proposed an oxidation process of CH_4 by N_2O similar to (R1), but suggested a further oxidation of Fe–OCH_3 by N_2O, different from (R2), to generate CO and recover the active site:

$$Fe{-}OCH_3 + 2N_2O \rightarrow Fe{-}OH + CO + H_2O + 2N_2 \quad (R5)$$

Thus, the sum reaction equation is:

$$3N_2O + CH_4 \rightarrow CO + 3N_2 + 2H_2O \quad (R6)$$

These two mechanisms have been supported by our above observations that both CO and CO_2 are generated (Figs. 3 and 7) in a way depending on the CH_4/N_2O ratio and NO concentration. When the CH_4/N_2O ratio increases, more CO while less CO_2 are generated, i.e. the contribution of (R5) becomes more significant while (R2) and (R3) have less contribution to N_2O–CH_4 SCR (Fig. 3). This is probably attributed to the fact that partial reduction of CH_4 at a higher concentration is enough to facilitate N_2O decomposition.

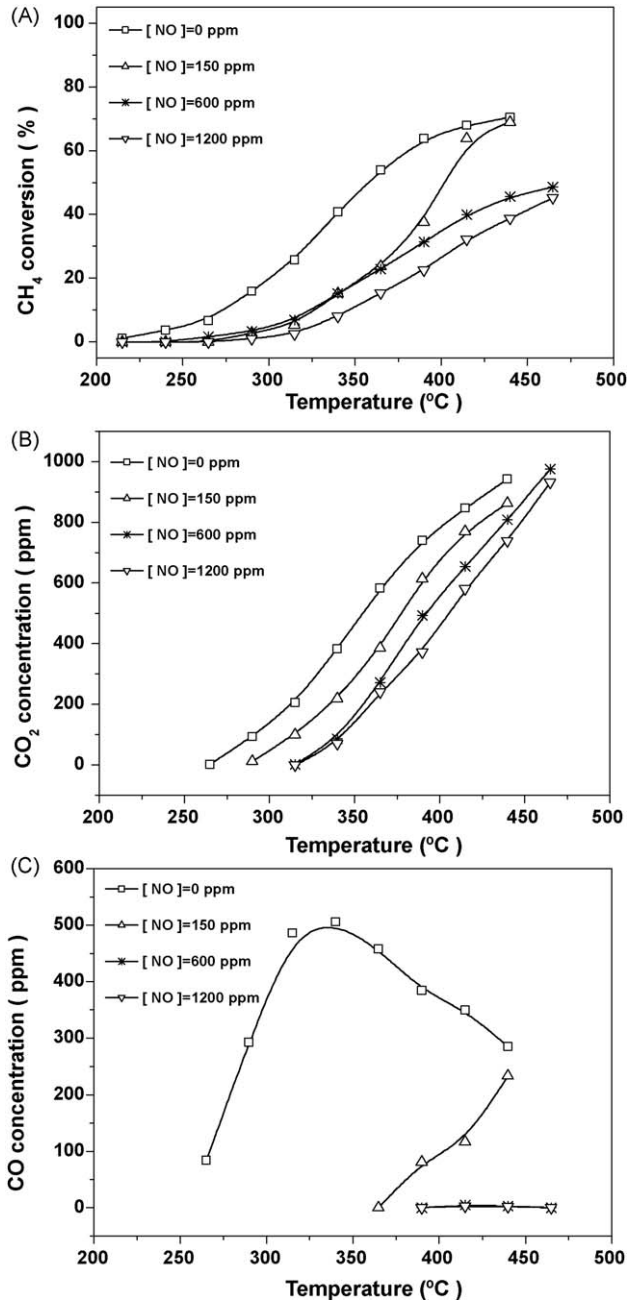

Fig. 7. (A) CH_4 consumption profile; (B) CO_2 and (C) CO profiles formed in N_2O-SCR by CH_4 under reaction conditions: 0.10 g catalyst; 5000 ppm N_2O, 1750 ppm CH_4; 0, 150, 600, or 1200 ppm NO; balance He; GHSV = 30,000 h^{-1}.

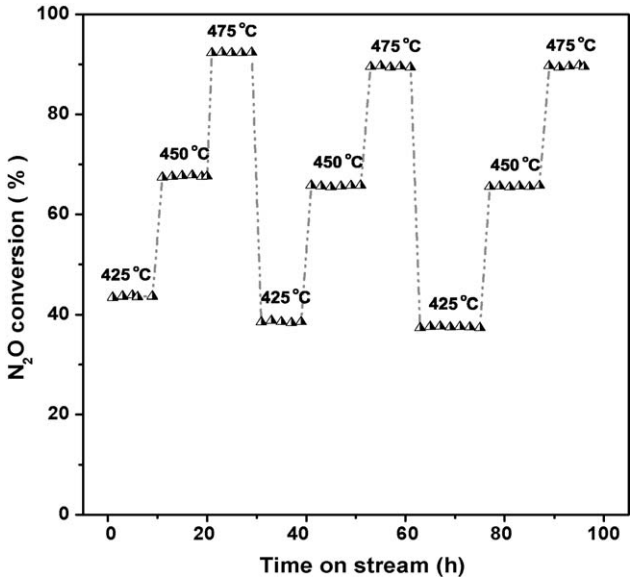

Fig. 8. Time on stream behavior of Fe-USY catalyst for N_2O–CH_4 SCR under reaction conditions: 0.10 g catalyst; 5000 ppm N_2O; 1750 ppm CH_4; 700 ppm NO; 5% O_2, 2% H_2O, balance He; GHSV = 30,000 h^{-1}.

When NO concentration increases, both CO and CO_2 concentrations decrease (addressed shortly).

In addition, the CO profile (Fig. 3D) indicates that the increase of CO concentration is declined at above 300 °C, which is ascribed to CO participation in reducing N_2O as shown in Fig. 1. As the temperature increases, more CO participate N_2O reduction, i.e. N_2O–CO SCR, which causes a maximum CO concentration at 325 °C ($CH_4/N_2O = 0.20$) and complete consumption of CO (freshly generated in (R5)) for N_2O-SCR at >375 °C. In the cases of $CH_4/N_2O = 0.25$, 0.35 (Fig. 7C) and 0.50, the amount of CO generated in (R5) is too high to be completely consumed even at 450 °C.

4.2. The effect of O_2 on N_2O–CH_4 SCR

The inhibition of N_2O–CH_4 SCR by O_2 has been reported [21] and also observed in Fig. 4. For direct N_2O decomposition, O_2 molecules can occupy the iron active sites via the oxygen chemisorption and then inhibit the combination of two active oxygen atoms on the surface. In the case of N_2O–CH_4 SCR, the inhibition of O_2 probably undergo its reaction with the intermediates in competition with N_2O, apart from the above-mentioned occupation effect of O_2:

$$Fe{-}OCH_3 + 1.5O_2 \rightarrow Fe{-}OH + CO_2 + H_2O \quad (R7)$$

$$Fe{-}OOCH + 0.5O_2 \rightarrow Fe{-}OH + CO_2 \quad (R8)$$

Although (R7) is not favored as (R2), (R8) is very much competitive to (R3), as observed by Nobukawa et al. [28]. The occurrence of (R8) and (R7) has also been supported by our own observations. Fig. 9 shows the relationship between the formed CO_2 concentration and the decomposed N_2O concentration in various mixture systems. The dotted line (the slope = 0.25) describes the theoretical situation (R4). Note that the lines representing the cases in $N_2O + CH_4$, $N_2O + CH_4 + NO$ and $N_2O + CH_4 + NO + O_2$ are almost superposed and located below the dotted line. This implies that part CH_4 is converted to CO. However, in $N_2O + CH_4 + O_2$ mixture, the line is above the dotted line and steeper (the slope = 0.39), indicating that more than stoichiometric CO_2 is produced. For example, when 100% 5000 ppm N_2O is decomposed, the detected CO_2 concentration is *ca.* 1800 ppm, far more than the stoichiometric concentration (1250 ppm), but nearly the same as the CH_4 concentration (1750 ppm). Therefore, the more generated CO_2 amount is produced through oxidation of the intermediates by O_2, which is more obvious at a higher N_2O conversion, i.e. at a higher temperature.

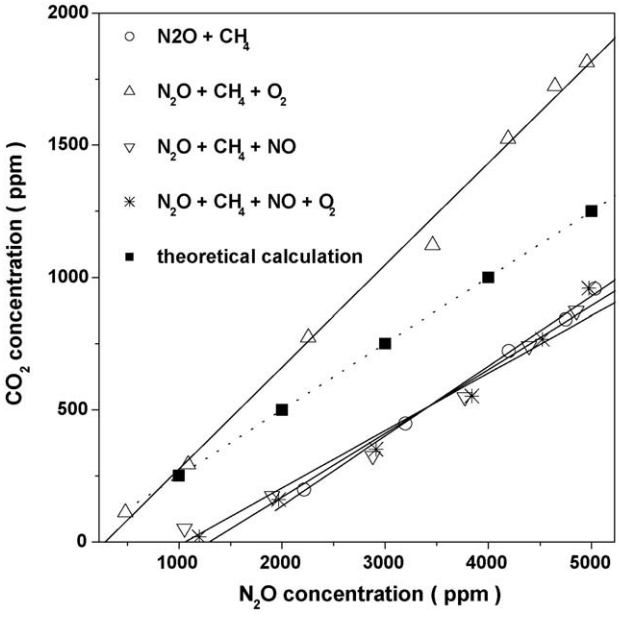

Fig. 9. Relationship between the formed CO_2 concentration and the decomposed N_2O concentration under reaction conditions: 0.10 g catalyst; 5000 ppm N_2O; 1750 ppm CH_4; 700 ppm NO; and/or 5% O_2; balance He; GSHV = 30,000 h^{-1}.

4.3. The effect of NO on N_2O–CH_4 SCR

Pirngruber et al. reported that the presence of small amount of NO can lead to significant promotion of direct N_2O decomposition over Fe–zeolite catalysts [32,33], and attributed to facilitation of the recombination of two surface active oxygen atoms via following pathways:

$$*{-}O + NO \rightarrow *{-}NO_2(ad) \quad (R9)$$

$$*{-}NO_2(ad) \rightarrow * + NO_2 \quad (R10)$$

$$NO_2 + *{-}O \rightarrow * + NO + O_2 \quad (R11)$$

Our previous experiments have supported the above mechanism as an essential amount of NO_2 is detected in the outlet stream in NO-assisted N_2O decomposition over Fe-USY catalyst (not shown here). However, opposite to the positive effect in direct N_2O decomposition, NO shows a negative effect on N_2O–CH_4 SCR (Fig. 4). The similar observation has been reported elsewhere for HC-SCR and CO SCR of N_2O [34,35]. For example, the N_2O conversion at temperatures of 375 and 425 °C is reduced from *ca.* 70% and 100% in C_3H_8-SCR of N_2O to *ca.* 15% and 50% in the presence of NO [34], respectively. Pérez-Ramírez et al. [35] reported that increasing the partial NO pressure in the $N_2O + C_3H_8 + O_2$ system gradually moves the reaction mechanism from N_2O-SCR to NO-assisted N_2O decomposition, which, in our belief, is also happening in N_2O+CH_4+NO system when [NO] is varied in 150–1200 ppm.

First of all, NO molecules strongly occupy the active sites so that N_2O–CH_4 SCR is prohibited to a larger extent even NO concentration is only 150 ppm (R9). As shown for NO-TPD over Fe-USY catalyst in Fig. 10A, the main desorption appears in 150–350 °C, tentatively assigned to the physically/chemically adsorbed NO (R9). We further monitored the NO and NO_2 concentrations in TPD by flowing the $N_2O + CH_4 + NO$ mixture over Fe-USY catalyst, as shown in Fig. 10B. Noted that a NO desorption peak appears in 150–350 °C, the same as in NO-TPD. When the temperature increases to over 350 °C, an NO consumption in 350–480 °C is observed, similar to the NO concentration profile in NO-assisted N_2O decomposition [32]. In 350–400 °C, the NO decrease is observed, which is tentatively attributed to the reaction of NO with *–O to form NO_2 ((R9) and (R10)). When the temperature is increased to 400–480 °C, the NO concentration is gradually recovered to the inlet concentration (R11) and kept invariable afterwards. Correspondingly, the NO_2 concentration is gradually increased to a maximum value in 300–350 °C but decreased all along and finally disappears in 500–600 °C (Fig. 10B), which is also consistent with the NO_2 profile in NO-assisted N_2O decomposition (Supplementary Figure S3).

More importantly, as shown in Figs. 6 and 7, the higher NO partial pressure leads to less CH_4 consumed and less CO and CO_2 generated while the N_2O conversion profile is not much different. This is because the strong occupation of active sites by NO reduces the active sites number available for N_2O–CH_4 SCR and inhibits N_2O–CH_4 SCR. In particular, at [NO] ≥600 ppm, the freshly produced CO is so little that it is consumed immediately via joining N_2O-SCR and no CO detected (Fig. 7C). Thus, apart from N_2O–CH_4 SCR, NO-assisted N_2O decomposition and N_2O–CO SCR have also some contribution to N_2O conversion to in $N_2O + CH_4 + NO$ system.

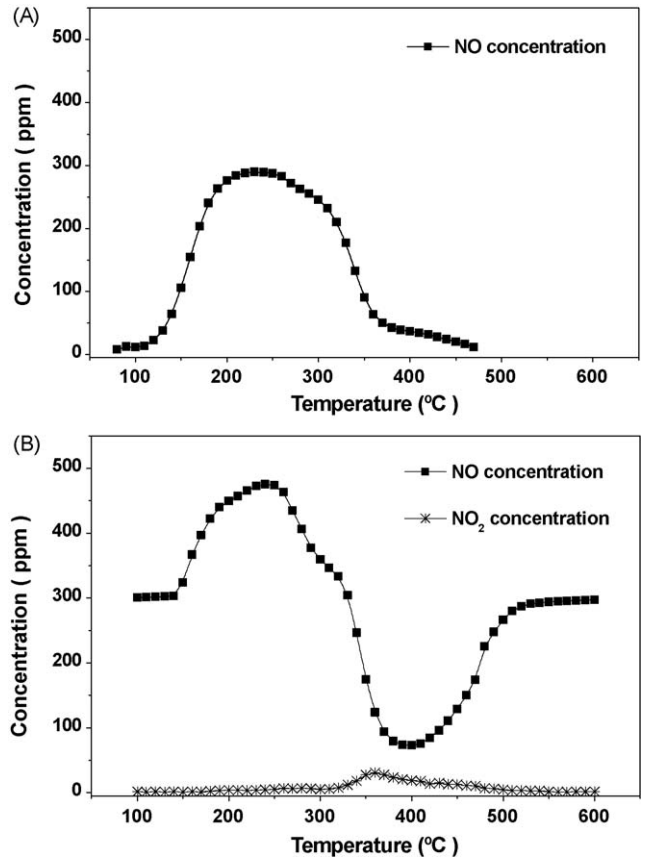

Fig. 10. TPD of NO over Fe-USY when purging with (A) He and (B) 5000 ppm N_2O; 1750 ppm CH_4 and 300 ppm NO in He at a heating rate of 5 °C min^{-1} from 100 to 600 °C.

Furthermore, our experiments demonstrate that a higher NO partial pressure leads to more O_2 generated (Supplementary Figure S4). The possible reaction pathway that produces O_2 in $N_2O + CH_4 + NO$ includes NO and N_2O direct decomposition, and NO-assisted N_2O decomposition. Fig. 10B indicates that the NO concentration becomes the same as the inlet concentration at the temperature >500 °C, which suggests no NO direct decomposition happening in this temperature range. In addition, N_2O direct decomposition is inhibited in the presence of H_2O which is freshly produced from $N_2O + CH_4$ reaction in our previous studies [11,12]. Thus, NO-assisted N_2O decomposition is the main reaction responsible for O_2 formation (R11).

In brief, in terms of the reaction product distribution (O_2, CO and CO_2), the effect of NO on N_2O–CH_4 SCR seems to gradually inhibit N_2O–CH_4 SCR and prefers NO-assisted N_2O decomposition. We believe that the two mechanisms are additive in some way to affect the N_2O decomposition and product distribution.

5. Conclusion

In this research, N_2O reduction by CH_4 has been systematically investigated over Fe-USY catalyst with the interference of NO and O_2. The presence of NO, O_2 and H_2O all has a negative effect on N_2O–CH_4 SCR, where the NO effect is the most severe. In N_2O–CH_4 SCR, the freshly formed CO can be further oxidized to CO_2 by N_2O, i.e. N_2O–CO SCR jointly decomposes N_2O at temperatures >300 °C. The O_2 inhibition of the N_2O conversion is mainly attributed to O_2 participation in oxidizing the intermediate species. The inhibition of NO on N_2O–CH_4 SCR, the stoichiometric relationship between the produced CO/CO_2 and the converted N_2O and CH_4 amount, and the amount of CO, CO_2 and O_2 suggest that N_2O decomposition in $N_2O + CH_4 + NO$ system combines three pathways: N_2O–CH_4 SCR, N_2O–CO SCR, and NO-assisted N_2O decomposition.

Acknowledgements

This work was financially supported by National Natural Science Fund of China (20725723, 20703057) and National Basic Research Program of China (2004CB719500). The support from the ARC Centre for Functional Nanomaterials funded by the Australia Research Council under its Centre of Excellence Scheme is also appreciated.

Appendix A. Supplementary data

Supplementary data associated with this article can be found, in the online version, at doi:10.1016/j.apcatb.2009.05.034.

References

[1] H. Rodhe, Science 248 (1990) 1217.
[2] IPCC, Climate Change (IPCC), 2001.
[3] N. Russo, D. Fino, G. Saracco, V. Specchia, Catal. Today 119 (2007) 228–232.
[4] N. Russo, D. Mescia, D. Fino, G. Saracco, V. Specchia, Ind. Eng. Chem. Res. 46 (2007) 4226–4231.
[5] J.P. Dacquin, C. Dujardin, P. Granger, J. Catal. 253 (2008) 37–49.
[6] J. Haber, M. Nattich, T. Machej, Appl. Catal. B 77 (2008) 278–283.
[7] G.D. Pirngruber, J. Catal. 219 (2003) 456–463.
[8] J.-H. Park, J.-H. Choung, I.-S. Nam, S.-W. Ham, Appl. Catal. B 78 (2008) 342–354.
[9] P.J. Smeets, Q.G. Meng, S. Corthals, H. Leeman, R.A. Schoonheydt, Appl. Catal. B 84 (2008) 505–513.
[10] P.J. Smeets, B.F. Sels, R.M. van Teeffelen, H. Leeman, E.J.M. Hensen, R.A. Schoonheydt, J. Catal. 256 (2008) 183–191.
[11] L.D. Li, Q. Shen, J.J. Yu, Z.P. Hao, Z.P. Xu, G.Q. Max Lu, Environ. Sci. Technol. 41 (2007) 7901–7906.
[12] L.D. Li, Q. Shen, J.J. Li, Z.P. Hao, Z.P. Xu, G.Q. Max Lu, Appl. Catal. A 314 (2008) 131–141.
[13] Q. Shen, L.D. Li, Z.P. Hao, Z.P. Xu, Appl. Catal. B 84 (2008) 734–741.
[14] M.N. Debbagh, C. Salinas Martínez de Lecea, J. Pérez-Ramírez, Appl. Catal. B 70 (2007) 335–341.
[15] A. Ates, Appl. Catal. B 76 (2007) 282–290.
[16] T. Nobukawa, M. Yoshida, K. Okumura, K. Tomishige, K. Kunimori, J. Catal. 229 (2005) 374–388.
[17] A. Guzmán-Vargas, G. Delahay, B. Coq, Appl. Catal. B 42 (2003) 369–379.
[18] M.N. Debbagh, A. Bueno-López, C. Salinas Martínez de Lecea, J. Pérez-Ramírez, Appl. Catal. A 327 (2007) 66–72.
[19] S. Kawi, S.Y. Liu, S.-C. Shen, Catal. Today 68 (2001) 237–244.
[20] G. Delahay, M. Mauvezin, B. Coq, S. Kiegery, J. Catal. 202 (2001) 156–162.
[21] S. Kameoka, K. Kita, T. Takeda, S. Tanaka, S. Ito, K. Yuzaki, T. Miyadera, K. Kunimori, Catal. Lett. 69 (2000) 169–173.
[22] S. Kameoka, T. Suzuki, K. Yuzaki, T. Takeda, S. Tanaka, S. Ito, T. Miyadera, K. Kunimori, Chem. Commun. 9 (2000) 745–746.
[23] M.N. Debbagh Boutarbouch, J.M. García Cortés, M. Soussi El Begrani, C. Salinas Martínez de Lecea, J. Pérez-Ramírez, Appl. Catal. B 54 (2004) 115–123.
[24] J. Pérez-Ramírez, J. Catal. 227 (2004) 512–522.
[25] T. Nobukawa, M. Yoshida, S. Kameoka, S. Ito, K. Tomishige, K. Kunimori, Catal. Today 93–95 (2004) 791–796.
[26] T. Nobukawa, K. Sugawara, K. Okumura, K. Tomishige, K. Kunimori, Appl. Catal. B 70 (2007) 342–352.
[27] S. Kameoka, T. Nobukawa, S. Tanaka, S. Ito, K. Tomishige, K. Kunimori, Phys. Chem. Chem. Phys. 5 (2003) 3328–3333.
[28] T. Nobukawa, M. Yoshida, S. Kameoka, S. Ito, K. Tomishige, K. Kunimori, J. Phys. Chem. B 108 (2004) 4071–4079.
[29] J.N. Armor, Catal. Today 26 (1995) 147–158.
[30] A. Ribera, I.W.C.E. Arends, S. de Vries, J. Pérez-Ramírez, R.A. Sheldon, J. Catal. 195 (2000) 287–297.
[31] B.R. Wood, J.A. Reimer, A.T. Bell, M.T. Janicke, K.C. Ott, J. Catal. 225 (2004) 300–306.
[32] G.D. Pirngruber, J.A.Z. Pieterse, J. Catal. 237 (2006) 237–247.
[33] J. Pérez-Ramírez, F. Kapteijn, G. Mul, J.A. Moulijn, J. Catal. 208 (2002) 211–223.
[34] M.A.G. Hevia, J. Pérez-Ramírez, Appl. Catal. B 77 (2008) 248–254.
[35] J. Pérez-Ramírez, F. Kapteijn, Appl. Catal. B 47 (2004) 177–187.